ELSEVIER

Journal of Hazardous Materials B72 (2000) 39–52

Journal of Hazardous Materials

www.elsevier.nl/locate/jhazmat

Correlation model to predict residual immiscible organic contaminants in sandy soils

Lizette R. Chevalier [a,*], Jeannette M. Fonte [b]

[a] *Department of Civil Engineering, MC 6603, Southern Illinois University Carbondale, Carbondale, IL 62901-6603, USA*

[b] *Ecological Systems, Indianapolis, IN 46218, USA*

Received 5 April 1999; received in revised form 23 July 1999; accepted 20 September 1999

Abstract

Researchers in both environmental and petroleum engineering have conducted studies in one-dimensional columns to quantify the amount of residual nonaqueous phase liquids (NAPL) trapped in the porous media as a function of capillary, viscous and buoyancy forces. From these previous studies, it is proven that significant amounts of the original NAPL spill remain as a trapped residual. The objective of this research was to extend this body of work and to develop a correlation model that could predict residual NAPL saturation as a function of common soil characteristics and fluid properties. These properties include parameters derived from sieve analysis, namely, the uniformity coefficient (C_u), the coefficient of gradation (C_c), as well as fluid properties (interfacial tension, viscosity and density). Over 100 column experiments were conducted across a range of nine different soil gradations. The data produced by these tests, along with measured soil and fluid properties, were used to generate correlation models to predict residual NAPL saturation (S_{rn}). The first correlation model predicts S_{rn} for the region where residual NAPL saturation is independent of the capillary number, and dependent on C_u, C_c and the Bond number. The second correlation model predicts S_{rn} for the region where residual NAPL saturation is dependent on capillary number, as well as C_u, C_c and the Bond number. The third correlation model predicts S_{rn} over the entire region as a function of C_u, C_c and the total trapping number. The correlation models have a R^2 value of 0.972, 0.934 and 0.825, respectively. Hence, the models may potentially be integrated into site characterization approaches.

Keywords: NAPL; Groundwater; Residual trapping; Soil contamination; Hydrocarbons; Laboratory investigation

* Corresponding author. Tel.: +1-618-453-6648; fax: +1-618-453-3044; e-mail: cheval@engr.siu.edu

0304-3894/00/$ - see front matter
PII: S0304-3894(99)00157-0

1. Introduction

Releases of nonaqueous phase liquids (NAPL) result from accidental spills, improper disposal and leaking underground storage tanks and pipes. Although immiscible with groundwater, NAPL contaminants pose a threat to aquifers due to mass transfer or partitioning into the aqueous and air phases. A NAPL denser than water (DNAPL) has the potential to migrate through the vadose zone and the saturated region. As it migrates, DNAPL may become trapped in the saturated zone as a discontinuous or residual phase due to capillary forces stronger than the opposing buoyancy (gravitational) and viscous forces. In fact, large quantities of DNAPL released into the subsurface may become trapped as a residual unless a region of high permeability such as clay or rock impedes the migration. In this event, the DNAPL will pool as a highly saturated lens of NAPL above the impermeable layer. A NAPL less dense than water (LNAPL) has the potential to pool above the water saturated pores of the capillary fringe, as opposed to migrating further into the aquifer. As with the DNAPL lens, the pores within the LNAPL lens will be highly saturated.

During the summer and fall, high intensity rain and abundant vegetation decrease the amount of infiltration into the soil. As a result, the level of the water table decreases in an aquifer. However, during the winter and spring, it is not uncommon for a water table to rise five to 10 ft due to reduced vegetative growth and low intensity rains, both which promote infiltration as opposed to run-off. This seasonal rise of the water table may cause a lens of LNAPL released when the water table was low to become trapped as a discontinuous residual within the capillary fringe and below the water table for a significant portion of the year. In the case of both DNAPL and LNAPL, pumping to remove free product within a highly NAPL saturated lens cannot completely recover the NAPL. As with the rising water table or the DNAPL lens migration, NAPL will become trapped during pumping as a discontinuous residual.

Numerous studies, in both petroleum and environmental research, have measured the amount of NAPL trapping that occurs. Research by petroleum engineers provide the foundation of these studies that measure the residual saturation of NAPL (S_{rn}) as a function of dimensionless numbers comparing capillary, viscous and buoyancy forces [1–4]. This work predominantly evaluates trapping in consolidated sandstone and glass beads. The approach used by these studies was adapted to determine similar relationships in aquifer soils, namely, sandy soil (e.g. Ref. [5]). Numerous additional studies in both the petroleum literature and the environmental engineering literature report values of S_{rn} for various types of consolidated and unconsolidated materials. A broad summary of petroleum and environmental studies is presented by Mercer and Cohen [6] and Chevalier [7]. More recent research includes Pennell et al. [8] and Dawson and Roberts [9]. The common approach in all of these studies is to measure a single value of S_{rn}, or to develop a curve reporting the trend of S_{rn} as a function of the dimensionless numbers relating the ratio of viscous, capillary and buoyancy forces, namely, the capillary number, the Bond number and the total trapping number.

The overall objective of this research was to develop a correlation model to predict the amount of residual NAPL trapped based on capillary forces, viscous forces, buoyancy forces, soil properties and fluid properties. The first specific objective of this

research was to quantify the amount of residual NAPL in nine different gradations of soil subsequent to a range of displacement velocities. Over 100 column experiments were conducted, resulting in a set of curves to predict the S_{rn} vs. the capillary number, with each of these curves representing a unique value of the coefficient of gradation, the uniformity coefficient, the Bond number and the total trapping number. The second specific objective was to analyze the relationships between these parameters and the resulting saturation of residual NAPL in order to develop a correlation model to predict trapping.

2. Background

The terminology for variably saturated soils has not been developed in a consistent manner. Several terms have been used to define an immiscible fluid surrounded by water in the porous space of soils. These terms include ''entrapped'', ''residual'', ''trapped'' and ''nucleated'' [10]. In addition, the term residual has been used to refer to NAPL in the vadose zone, which may or may not be continuous. This research is focused on discontinuous NAPL in previously water saturated soils found below the upper region of the capillary fringe. The term *residual* will be used, and the saturation of residual NAPL will be referred to as S_{rn}.

In a hydrophilic soil, NAPL is the non-wetting fluid, whereas water is the wetting fluid. The non-wetting fluid can become trapped as a residual as a result of snap-off or by-passing as the wetting fluid imbibes into soils where the two phases were previously continuous [3,4]. The factors which determine the mechanisms of trapping include the geometry of the pore network, fluid properties (interfacial tension, density and viscosity), the applied pressure gradient and gravity [1]. These factors are integrated into dimensionless numbers that relate the ratio of viscous, buoyancy (gravitational) and capillary forces.

The capillary number, *Nc*, relates the ratio between viscous and capillary forces [1]:

$$Nc = \frac{\nu\mu}{\sigma} \tag{1}$$

where ν is velocity of the aqueous phase, μ is the viscosity of the aqueous phase and σ is interfacial tension between the immiscible phases. The Bond number, *Nb*, relates the ratio between buoyancy (gravitational) and capillary forces [1]:

$$Nb = \frac{\Delta\rho g R^2}{\sigma} \tag{2}$$

where $\Delta\rho$ is the difference in density between the immiscible fluids, g is the gravitational constant and R is a characteristic soil dimension, such as the mean grain size diameter. *Nb* has also been defined as a function of intrinsic permeability, k [1]:

$$Nb = \frac{\Delta\rho g k}{\sigma} \tag{3}$$

In these equations, the contact angle is assumed to be zero. Morrow and Songkran further define the relationship between the two definitions of Nb (defined as $Nb_{(R^2}$ and $Nb_{(k)}$) by recognizing that the k can be expressed in terms of R through the Kozeny–Carman's equation:

$$k = \frac{n^3}{K_z(1-n)^2 A_s^2} \tag{4}$$

where A_s is the specific surface area per unit solid volume $(3/R)$, K_z is the Kozeny constant, which by experiment has been shown to be approximately equal to 5 for well-sorted sands or sphere packings, and n is porosity, which is usually equal to about 0.389 for random packings of equal spheres. Substitution of these values in Eq. (4) gives an approximate relationship between k and R for a random packing of equal spheres:

$$k = 0.00317R^2 \tag{5}$$

It follows that the relationship between Eqs. (2) and (3) is:

$$Nb_{(k)} = 0.00317Nb_{(R^2)} \tag{6}$$

Pennell et al. [8] included relative permeability (k_{rw}) in the Bond number $(\Delta\rho gkk_{rw}/\sigma)$. Dawson and Roberts [9] included porosity (n) in the Bond number $(\Delta\rho gk/n\sigma)$. In both equations, the additional term is dimensionless with a value less than one, which in most cases would change $Nb_{(k)}$ by an order of magnitude (decrease or increase, respectively).

Morrow and Songkran [1] evaluated the effects of $Nb_{(R^2)}$ and Nc using glass beads over a wide range of mesh sizes (12–115). Among other factors, they investigated the correlation of the combined effects of gravity and viscous forces to overcome capillary forces. They determined that residual saturation correlated to a simple linear combination of $Nb_{(R^2)}$ and Nc, which was referred to as the total trapping number:

$$N_{t(1)} = Nc + 0.001412\,Nb_{(R^2)} \tag{7}$$

Higher values of N_t correspond to lower saturations of S_{rn}. Pennell et al. [8] derived a total trapping number for both horizontal and vertical flow based on $Nb_{(k)}$

$$N_{t(2)} = \sqrt{Nc^2 + Nb_{(k)}^2} \quad \text{(horizontal)} \tag{8}$$

$$N_{t(3)} = |Nc + Nb_{(k)}| \quad \text{(vertical)} \tag{9}$$

Substituting Eq. (6) into Eq. (9) results in an equation within the same order of magnitude as Eq. (7). Using $Nb_{(k)}$, Pennell et al. [8] graphed S_{rn} as a function of $Nb_{(k)}$, Nc and $N_{t(3)}$, showing that $Nb_{(k)}$ is in general an order of magnitude more than Nc in the dynamic range of the reducing S_{rn} (e.g., where S_{rn} is reduced as $Nb_{(k)}$, Nc and N_t increase). If $Nb_{(R^2)}$ was used, evidence of the stronger influence of buoyancy forces over capillary forces would have been reverse.

Pennell et al. [8] evaluated the mobility of residual NAPL, over a range of soils while using surfactants to reduce interfacial tension (i.e. increasing $Nb_{(k)}$, Nc and N_t). By first trapping NAPL in soil columns, they were able to show that mobility of residual NAPL can be enhanced using surfactant flushing at greater levels than through water flushing alone.

Dawson and Roberts [9] evaluated the mobility of NAPL up until the point of NAPL becoming trapped as a discontinuous residual. They evaluated different NAPL compounds, which allows them to use a range of *Nc* through changes in interfacial tension as well as velocity. In addition, they consider different approaches in water flooding, comparing horizontal flow to vertical and angled flow.

The work presented in this paper, in contrast, evaluated the range of residual saturation (trapping) that occurred due to changes in viscous, buoyancy and capillary forces, which in part extends the work of Dawson and Roberts [9]. Because it evaluates the amount of NAPL originally trapped, it is also distinctly different from the work of Pennell et al. [8] evaluating the mobilization of trapped residual NAPL.

Sieve analysis classifies a soil by the percentage of total weight of soil that passes through different sieves, and is used to generate particle size distribution curves. Parameters determined by the curves are used to classify soils. By convention, the grain size D is given a subscript to identify the percent of finer material. For example, the diameter particle size corresponding to 10% finer is referred to as D_{10}, which is also the effective grain size [11]. The uniformity coefficient, C_u, is calculated as:

$$C_u = \frac{D_{60}}{D_{10}} \tag{10}$$

The coefficient of gradation, C_c, is calculated as:

$$C_c = \frac{D_{30}^2}{D_{60} \times D_{10}} \tag{11}$$

This coefficient gives a measure of the shape of the curve between D_{60} and D_{10}. A soil in which most of the soil grains are the same size is described as uniform or poorly graded, as opposed to a soil in which the particles sizes are distributed over a wide range, which is termed non-uniform or well-graded [11,12].

3. Materials and methods

A 15-cm borosilicate glass column manufactured to minimize sorption losses and to maintain a hydrophillic surface was used in this study (Kontes Model 420830-1520). All surfaces are made of glass or teflon (PTFE).

The soil used for the first seven sets of experiments were several grades of 4010 industrial quartz, fine silica sand from the Unimin (Associated Lumber, Carbondale, IL). This stock sand, which is referred to as Fine Silica Stock (FS Stock), was used in a set of experiments. Six other gradations were defined from sieving the FS Stock. The objective behind mixing the different meshes within the FS Stock was to achieve varying soil characteristics (i.e. C_u and C_c). Fine Silica Mix 1 (FS Mix 1) was obtained by sieving the FS Stock and removing the fines passing through a 70-mesh sieve. FS Mix 2 was obtained by combining 90% of FS Mix 1 with 10% of 100 mesh soil (the sand passing the 70-mesh sieve and retained on the 100-mesh sieve). FS Mix 3 was obtained by combining 80% of FS Mix 1 with 20% of 100 mesh soil. FS 50 was

composed of the sand passing the 40-mesh sieve and retained on the 50-mesh sieve. FS Mix 4 was obtained by combining 30% of FS Mix 1, 10% of FS 50, 30% of 70 mesh (the sand passing the 50-mesh sieve and retained on the 70-mesh sieve), 20% of 80 mesh (the sand passing the 70-mesh sieve and retained on the 80-mesh) and 10% of 100 mesh (the sand passing the 80-mesh sieve and retained on the 100-mesh sieve). FS Mix 5 was obtained by combining 10% of FS 50, 70% of 70 mesh, 5% of 80 mesh and 15% of 100 mesh.

The second porous media used for the 8th and 9th sets of experiments were two different grades of a filtration sand and gravel (coarse silica sand) from the Unimin. This stock sand, which is referred to as Coarse Silica Stock (CS Stock), was used in a set of experiments. Coarse Silica 20 (CS 20) was obtained by sieving the CS Stock and collecting the sand passing through a 16-mesh sieve and retained on the 20-mesh sieve. The sieve analysis of all nine of the soil gradations was performed after they were mixed according to ASTM C 136.

The wetting phase used in these experiments was distilled, deionized, deaired water. The water was distilled and deionized with a Corning Mega-pure system. Wilson et al. [5] conducted similar experiments for a range of NAPLs, and determined that S_{rn} was largely independent of the organic liquid used. Hence, Soltrol was selected as a representative NAPL contaminant based on the desirable physical properties of low solubility and low volatility. These properties allowed us to limit the mass transfer that occurs into the air and water phases and to focus our study on the entrapment of the immiscible phase. To observe the immiscible fluid movement and entrapment, a red oil soluble dye was used to dye the Soltrol (Oil Red O biological stain, Aldrich, Milwaukee, WI).

Interfacial tension measurements were conducted using a Fisher Scientific Tensiomat 21 du Nouy ring tensiometer. The interfacial tension between dyed Soltrol and pore water was determined to be 40.3 ($\pm$4.5%) dyn/cm. (Note: values reported in parenthesis are the coefficient of variation). Viscosity was measured using a Gilmont falling ball viscometer. The viscosity of dyed Soltrol was determined to be 4.08 ($\pm$0.14%) cp. The density of the dyed Soltrol was determined to be 0.775 ($\pm$0.12%) g/cm^3. All measurements were conducted at 24°C. The use of dye had no discernable effect on the flow or trapping of residual NAPL.

The method for preparing the water saturated column and simulating naturally occurring aquifer condition that would trap NAPL is reported by Chevalier [7]. In summary, a soil column was saturated from the bottom under vacuum with deionized deaired water to prevent the entrapment of air as a non-wetting fluid. The column was then flushed from the top with NAPL to assure a stable displacement of the aqueous phase [13]. Once the NAPL reached the bottom of the column, the flow of NAPL was interrupted. The aqueous flow was then reintroduced through the bottom of the column. The design of the system is shown in Fig. 1. Residual NAPL saturation (S_{rn}) was determined gravimetrically [5]. Of note, residual NAPL was observed in the soil pores near the wall using this procedure. When the column was disassembled, the residual NAPL was observed to be relatively uniformly distributed throughout the soil.

In order to trap a range of S_{rn}, *Nc* was varied by changing the velocity. The approximate range of velocities in aquifer environments during natural and remediation

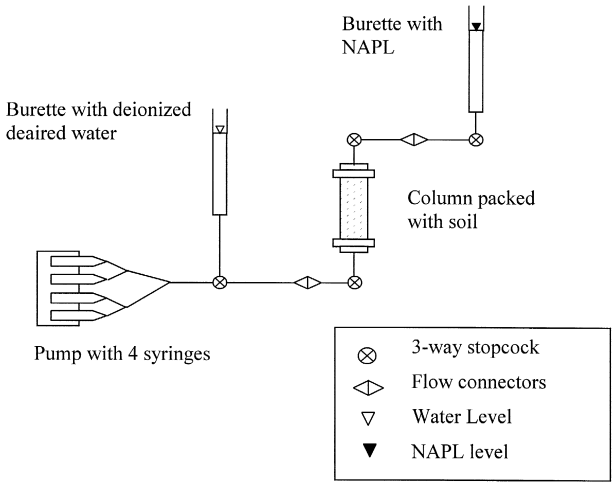

Fig. 1. Generalized schematic of experimental set-up.

conditions is 0.00046–0.0020 cm/s [14]. For the fluid used in this research, this would be equivalent to $1.03 \times 10^{-7} < Nc < 4.48 \times 10^{-7}$. However, S_{rn} is independent of Nc at approximately $Nc < 10^{-6}$ [1]. Therefore, this range of velocities would theoretically produce the same value of S_{rn}. Assuming that remediation conditions referred to pumping to remove free product, higher velocities were considered, which established a trend in the data for regions where S_{rn} is dependent on Nc. This potentially relates to the used of surfactants and/or alcohols that reduce the interfacial tension (and subsequently increase Nc). The velocities used ranged from 0.0018 to 0.1842 cm/s, which results in $10^{-7} < Nc < 10^{-5}$. $Nb_{(R^2)}$ was used in the analysis, and hereinafter will be referred to as Nb. Nb was varied by using different soils, hence, changing R, the characteristic soil dimension, which in this study was D_{50}. The range of soil used resulted in 0.246 mm $< D_{50} <$ 0.975 mm which corresponds to $10^{-3} < Nb < 10^{-2}$. All measurements of S_{rn} were performed in triplicate. Regression analysis for the correlation model(s) was performed using SigmaPlot®.

4. Discussion

4.1. One-dimensional column trapping experiments

A new column was packed for each measurement of S_{rn}. A total of 108 columns were tested in order to develop nine sets of Nc–S_{rn} curves to ensure the robustness of the correlation models. A selected set of these curves are presented in Fig. 2. Each curve consists of four different capillary numbers, which were measured in triplicate for a total of 12 points. The darcy velocity was used to determine Nc. The average S_{rn} was plotted against Nc and a regression line was fit to these four data points. A typical curve, with

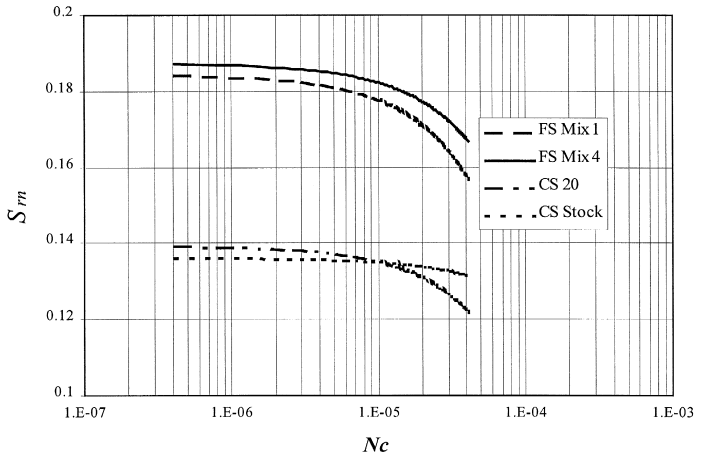

Fig. 2. $Nc-S_{rn}$ for select soils.

error bars, is shown in Fig. 3. In all of the curves, the expected trend, where S_{rn} decreased with increasing Nc, was achieved.

Fig. 2 also illustrates that S_{rn} is independent of Nc at approximately $Nc = 2 \times 10^{-6}$. This is similar to the results of other studies. Ng et al. [15] conducted a study using acrylic plastic beads and also found that S_{rn} is independent of Nc up to 2×10^{-5}. Morrow and Songkran [1] used glass beads and found that Nc had no effect on trapping up to 10^{-6}. Theoretically, this trend should continue for different soils.

In order to ensure the reliability and reproducibility of these experiments several different variables were analyzed, including the coefficients of variation between trials, (column) wall effects on porosity, and the Reynolds number. For each triplicate set of S_{rn} values, the coefficient of variation ranged from 0.02% to 5.36% with an average of 2.64%. This ensured that the results are consistent and reproducible. The residual water saturation, S_{rw}, was also measured to maintain experimental reproducibility as well as ensuring maximum NAPL saturation before flushing with water. The average coefficient of variation for S_{rw} was 6.07%.

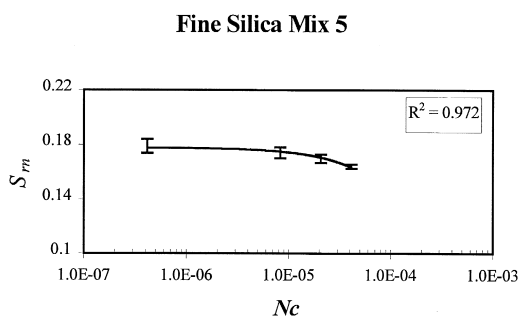

Fig. 3. Typical $Nc-S_{rn}$ curve developed, with corresponding error bars.

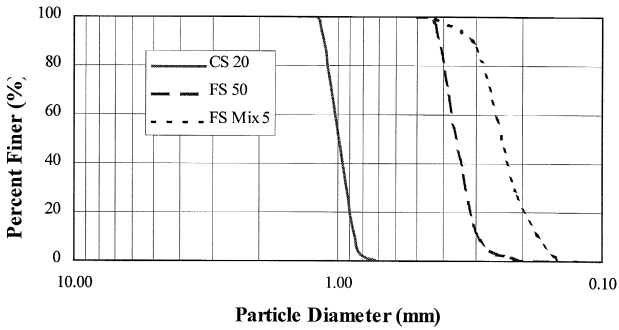

Fig. 4. Sieve analysis for select soils.

The effect of the column wall on packing and porosity was also investigated. Somerton and Wood [16] conducted a study to determine the wall effects on porosity in cylindrical and rectangular containers. By plotting porosity against the ratio of container diameter to particle diameter (D/d_p) a quadratic curve was fit to the data. At a ratio of 10:1, the estimated porosity is within 10% of the porosity for an infinite porous medium. For this research, the D/d_p ranged from 49:1 to 195:1. At these larger ratios, the porosities are estimated to be within 1% of that for an infinite medium and therefore are negligible. The Reynolds number was calculated to check for laminar flow conditions in the experiments using:

$$Re = \frac{\rho \nu d}{\mu} \tag{12}$$

where ν is the darcy velocity and d is the characteristic pore diameter (d_{50}). Darcy's law is only valid for laminar flow where the Reynolds number is less than 1–10 [17]. The Reynolds number was calculated for the nine soil mixtures at all four velocities and was found to range from 0.005 to 1.99. The Reynolds number was above 1.0 for only two of the 36 different runs.

Table 1
Summary of soil characteristics

Soil	D_{10}	D_{30}	D_{50}	D_{60}
FS Mix 1	0.332	0.385	0.418	0.434
FS Mix 2	0.284	0.357	0.423	0.402
FS Mix 3	0.234	0.325	0.381	0.407
FS Stock	0.237	0.320	0.371	0.395
FS 50	0.297	0.328	0.348	0.357
FS Mix 4	0.174	0.201	0.251	0.298
FS Mix 5	0.166	0.214	0.246	0.260
CS Stock	0.658	0.800	0.905	0.956
CS 20	0.876	0.935	0.975	0.994

Table 2
Summary of model variables

Soil	S_{rn}				C_u	C_c	$Nb_{(R^2)}$
	$Nc < 2E-06$	$Nc = 8.26E-06$	$Nc = 2.06E-05$	$Nc = 4.13E-05$			
FS Mix 1	0.184	0.179	0.171	0.157	1.309	1.030	9.67E−03
FS Mix 2	0.180	0.178	0.174	0.168	1.416	1.117	9.89E−03
FS Mix 3	0.182	0.180	0.175	0.167	1.738	1.110	8.01E−03
FS Stock	0.178	0.176	0.173	0.167	1.665	1.088	7.61E−03
FS 50	0.180	0.176	0.170	0.160	1.203	1.015	6.67E−03
FS Mix 4	0.187	0.183	0.177	0.167	1.708	0.782	3.49E−03
FS Mix 5	0.178	0.175	0.171	0.163	1.567	1.056	3.35E−03
CS Stock	0.136	0.135	0.134	0.131	1.453	1.019	4.53E−02
CS 20	0.139	0.136	0.131	0.122	1.135	1.004	5.26E−02

4.2. Sieve analysis

The results of the sieve analysis are shown in Fig. 4 for a select number of the soil gradations used. Table 1 lists D_{10}, D_{30}, D_{50} and D_{60} for all nine soil gradations. These values were used to estimate C_u, C_d and Nb (Table 2). Of note, D_{50} was used to estimate Nb. The range of these parameters are $1.203 \leq C_u \leq 1.738$, $0.782 \leq C_c \leq 1.117$ and $3.35 \times 10^{-3} \leq Nb \leq 5.26 \times 10^{-2}$.

4.3. Development of correlation models

The regression package within SigmaPlot® graphing software was used to evaluate the correlation between independent (C_u, C_c, Nb, Nc and N_t) and dependent (S_{rn}) variables by estimating the coefficients of various models. The experimental values of S_{rn} at various Nc were obtained from the Nc–S_{rn} curves (Fig. 2). The independent variables, C_u, C_c and Nb were calculated from the soil properties in Table 1. Initial modeling efforts were focused on the region where S_{rn} is independent of Nc. The model

Table 3
Statistical attributes of fitted equations

Coefficient	Standard error	Coefficient of variation	Dependencies
Eq. (14): $R^2 = 0.972$			
−11.59	7.455E−01	6.430	0.2646
0.1824	1.361E−03	0.7463	0.2646
Eq. (15): $R^2 = 0.936$			
−10.58	5.770E−01	5.454	0.2645
0.1247	7.602E−04	0.6097	0.2645
Eq. (16): $R^2 = 0.824$			
0.0371	4.425e−3	11. 1	0.994
−0.1118	6.835e−2	61.16	0.892
0.1071	8.843e−2	82.54	0.060
−0.1417	1.183e−2	8.343	0.994

was then modified for the region where S_{rn} is dependent on *Nc*. A third model was developed using $N_{t(1)}$ as opposed to *Nb* and *Nc*. The statistical attributed of the fitted equations are summarized in Table 3.

Preliminary modeling was focused on obtaining the coefficients from an equation of the following form:

$$S_{rn} = aX_1^b X_2^c X_3^d \ldots X_i^n \tag{13}$$

where X_i's are independent variables, and all other variables coefficients determined through regression. Beyond this form, variations were considered using the ratios of various independent variables, as well as adding individual terms.

4.4. Model for S_{rn} independent of Nc

From the experimental data, it was shown that for $Nc < 2 \times 10^{-6}$, S_{rn} was independent of *Nc*. In this region, it was found that S_{rn} could be predicted as a function of C_u, C_c and *Nb* using the following expression:

$$S_{rn} = -11.59\left(\frac{C_u Nb}{C_c}\right)^2 + 0.182 \quad (R^2 = 0.972) \tag{14}$$

As stated earlier, *Nb* is determined using D_{50} as a characteristic length. The quality of fit of the model to the experimental data is presented in Fig. 5 where each data point represents the average of triplicate measurements (Table 2). Analysis of the residual between the experimental and estimated S_{rn} revealed no significant error trend related to the parameters C_c, C_u or *Nb* (Table 3). These results suggest that S_{rn} is affected by the physical properties of the soil and fluids. Because of the small range of soil gradations evaluated, Eq. (11) has limited application. However, it is reasonable to predict that the model could extend to other soils types, as well as other immiscible organic fluids. At a minimum, the strong correlation encourages additional study.

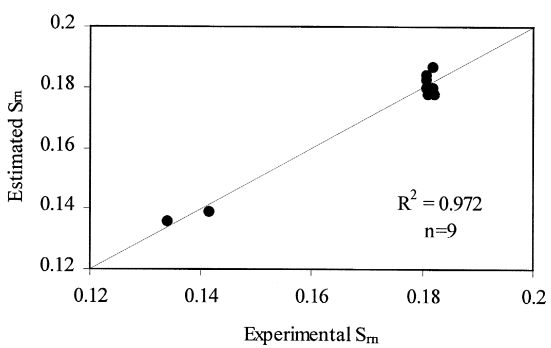

Fig. 5. Quality of fit for the model S_{rn} independent of *Nc* (Eq. (14)).

4.5. Model for S_{rn} dependent on Nc

Using the same general form as Eq. (14), a second model was developed for the region where S_{rn} is dependent on Nc ($2 \times 10^{-6} < Nc < 4.13 \times 10^{-5}$). S_{rn} data were obtained from the experimental curves at three different capillary numbers over the given range of interest. The correlation providing the best fit was determined to be:

$$S_{rn} = -10.58\left(\frac{C_u Nb}{C_c}\right)^2 + 0.1247Nc^{-0.03} \quad (R^2 = 0.934) \tag{15}$$

Eq. (15) allows a direct assessment of the impact of capillary and buoyancy forces for a system under investigation.

The quality of fit of the model to the experimental data is graphically depicted in Fig. 6. The assessment of these coefficients is given in Table 3. As with the previous model, analysis of the residual between the experimental and estimated S_{rn} reveals no significant error trend related to the parameters C_c, C_u, Nb or Nc. The R^2 value generated decreased from 0.972 to 0.934. Both models indicate that trapping is affected by soil and fluid properties.

4.6. Model for S_{rn} as a function of N_t

Regression was used to develop a correlation model as a function of $N_{t(1)}$, C_c and C_u. In this case, the entire range of S_{rn} was used. The correlation model providing the best fit was:

$$S_{rn} = 0.0371C_u^{-0.1118}C_c^{0.1071}N_{t(1)}^{-0.1417} \quad (R^2 = 0.824) \tag{16}$$

The quality of fit of the model to the experimental data is graphically depicted in Fig. 7. The assessment of these coefficients are listed in Table 3. As with the other models, the statistical analysis of the model suggest that it can be extended beyond the systems studied. When regression was performed on this equation using $N_{t(3)}$ (and hence $Nb_{(k)}$), R^2 was reduced to 0.709. Since three coefficients have a high dependency, two additional models were considered. In these two models, the terms C_u and C_c were

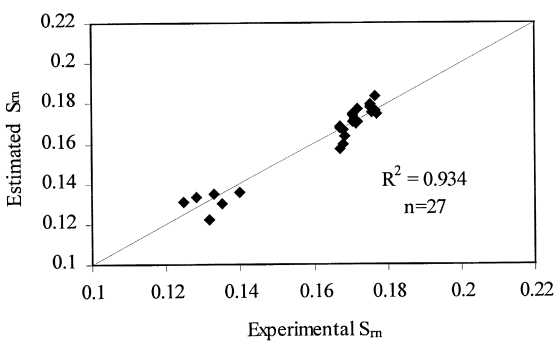

Fig. 6. Quality of fit for the model S_{rn} dependent of Nc (Eq. (15)).

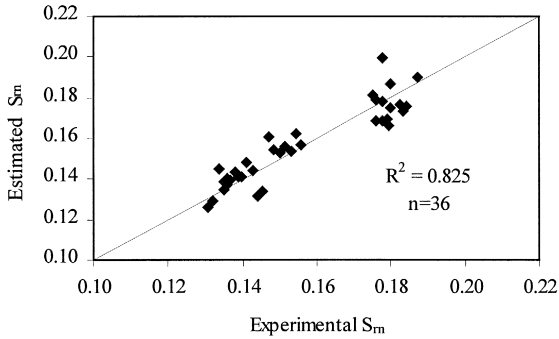

Fig. 7. Quality of fit for the model using N_t (Eq. (16)). $R^2 = 0.824$.

removed from Eq. (16). The R^2 in the resulting correlation models were 0.816 and 0.810, respectively, with no clear change in the dependency of the coefficients.

5. Conclusion

A family of curves was developed from experiments designed to measure S_{rn} as a function of *Nc*. Different soil types were used to develop these curves, resulting in a range of C_c, C_u and *Nb* values. Three correlation models were developed that reasonably predict S_{rn} from fluid and soil properties. One model is applicable at lower values of *Nc*, where S_{rn} is constant. The second model is applicable to the region where S_{rn} is dependent on *Nc*. The third model is applicable to both regions, and is a function of C_c, C_u, and N_t. The strong statistical correlation between the measured and predicted values of S_{rn} in all cases suggest that the models could be extended to include a wider range of soil mixtures, possibly including clay. In addition, the model theoretically should apply to different immiscible organic fluids. However, further testing is needed to test this inference.

Acknowledgements

Funding for this research was provided by grants from the Illinois Groundwater Consortium/USDA and the Materials Technology Center at Southern Illinois University Carbondale. The authors would like to thank Dr. Bruce DeVantier for his critique of the research. The constructive comments of anonymous reviewers were also appreciated.

References

[1] N.R. Morrow, B. Songkran, Effects of viscous and buoyancy forces on non-wetting phase trapping in porous media, in: D.O. Shah (Ed.), Surface Phenomena in Enhanced Oil Recovery, Plenum, New York, 1981.

[2] J.J. Taber, Research on enhanced oil recovery: past, present and future, in: D.O. Shah (Ed.), Surface Phenomenon in Enhanced Oil Recovery, Plenum, New York, 1981.
[3] N.C. Wardlaw, The effect of geometry, wettability, viscosity, and interfacial tension on trapping in single pore-throat pairs, J. Can. Pet. Technol. 21 (1982) 21–27.
[4] I. Chatzis, N.R. Morrow, H.T. Lim, Magnitude and detailed structure of residual oil saturation, SPEJ 23 (1983) 311–326.
[5] J.L. Wilson, S.H. Conrad, W.R. Hason, W. Peplinski, E. Hagen, Laboratory investigation of residual liquid organics from spills, leaks, and the disposal of hazardous wastes in groundwater, Robert S. Kerr Laboratory, Ada, OK, 1990, EPA/600/6-90/004.
[6] J.W. Mercer, R.M. Cohen, A review of immiscible fluids in the subsurface: properties, models, characterization and remediation, J. Contam. Hydrol. 6 (1990) 107–163.
[7] L.R. Chevalier, Evaluation of hydraulic controls to promote surfactant dissolution of trapped residual NAPL, PhD Dissertation, Michigan State University, Department of Civil and Environmental Engineering, 1994.
[8] K.D. Pennell, G.A. Pope, L.M. Abriola, Influence of viscous and buoyancy forces on the mobilization of residual tetrachloroethylene during surfactant flushing, Environ. Sci. Technol. 30 (1996) 1328–1335.
[9] H.E. Dawson, P.V. Roberts, Influence of viscous, gravitational and capillary forces on DNAPL saturation, Ground Water 35 (1997) 261–269.
[10] B.A. Faybishenko, Hydraulic behavior of quasi-saturated soils in the presence of entrapped air: laboratory experiments, Water Resour. Res. 31 (1995) 2421–2435.
[11] B.M. Das, Principles of Geotechnical Engineering, 4th edn., PWS Publishing, Boston, 1998.
[12] J.E. Bowles, Physical and Geotechnical Properties of Soils, 2nd edn., McGraw-Hill, 1984.
[13] B.H. Kueper, E.O. Frind, An overview of immiscible fingering in porous media, J. Contam. Hydrol. 2 (1988) 95–110.
[14] K.D. Pennell, L.M. Abriola, W.J. Weber, Surfactant enhanced solubilization of residual dodecane in soil columns: 1. Experimental investigation, Environ. Sci. Technol. 27 (1993) 2332–2339.
[15] K.M. Ng, H.T. Davis, L.E. Scriven, Visualization of blob mechanics in flow through porous media, Chem. Eng. Sci. 33 (1978) 1009–1017.
[16] C.W. Somerton, P. Wood, Effect of walls in modeling flow through porous media, J. Hydraul. Eng. 144 (1988) 1431–1448.
[17] C.W. Fetter, Applied Hydrogeology, 3rd edn., Prentice-Hall, 1994.